Siberian Branch of Russian Academy of Science

BUDKER INSTITUTE OF NUCLEAR PHYSICS

A. Bondar, A. Buzulutskov, L. Shekhtman,
A. Sokolov, A. Vasiljev

PERFORMANCE OF THE TRIPLE-GEM DETECTOR WITH OPTIMIZED 2-D READOUT IN HIGH INTENSITY HADRON BEAM

Novosibirsk
2001

Performance of the triple-GEM detector
with optimized 2-D readout
in high intensity hadron beam

A. Bondar, A. Buzulutskov, L. Shekhtman,

A. Sokolov, A. Vasiljev

Budker Institute for Nuclear Physics
630090 Novosibirsk, Russia

Abstract

Multiple-GEM detectors are considered to be good candidates for tracking devices in experiments with high hadronic background. We present the results of the triple-GEM detectors beam test in a high intensity pion beam. The detectors had an optimized two-dimensional readout with minimized strip capacitance. Such optimization permitted the starting point of the efficiency plateau down to a gain of 5000. The probability of GEM discharges induced by heavily ionizing particles has been measured as a function of gain: at a gain of 20000 it amounts to 10^{-11} per incident particle. Such a value will ensure safe operation of the detector in the conditions of forward region of the LHC experiments.

1 Introduction

Micro-pattern gas technologies have been considered as a good candidates for inner tracking systems of LHC experiments. A major problem of gas micro-pattern devices appeared to be heavily ionizing particles that are produced in nuclear interactions of hadrons with the material of the detectors. High and dense ionization produced in a sensitive region of the detector can provoke sparking with subsequent deterioration of its properties (gain and efficiency) and possible destruction. It was shown that introducing several gas amplification stages one can significantly improve performance of micropattern devices in this respect [1]. The most convenient and safe way of producing such multistage gas amlification was application of Gas Electron Multiplier (GEM)[2]. The last development in this direction, the Triple-GEM detector, utilizing 3 consequtive GEM foils was shown to be the most safe with respect to sparking in hadronic environment [3,4].

Triple-GEM detectors have been developed as a possible technology for the inner tracking in LHCb experiment [3,5]. Simulation of the LHCb interaction region, including the beam vacuum pipe, were performed to estimate the particle fluxes [6], using an average nominal luminosity of $2 \times 10^{32} \mathrm{cm}^{-2}\mathrm{s}^{-1}$. The particle fluxes and its compositions depend strongly on the position along the beam axis and on the distance from the beam. Maximum charged hadron rate is expected to be $8 \times 10^3 \, \mathrm{mm}^{-2}\mathrm{s}^{-1}$ and total hadron rate per station reaches 100 MHz. It was shown that the GEM foil can withstand more than 100 sparks per cm^2 without permanent damage[7]. If we require that sparking rate is limited to 1 per $10^3\mathrm{s}$ per tracking plane and take into account local and total hadronic rate, it follows that the discharge probability per incident particle must not exceed 10^{-11}.

In this paper we describe the Triple-GEM detector with optimized readout board. New readout allowed to reduce significantly interstrip capacitance and thus improve signal to noise ratio of the detector. The results of test in high intensity pion beam demonstrate considerable improvement in the performance related to discharges due to heavily ionizing particles.

3

2 Detector design and experimental set-up

The Triple-GEM detector consists of a primary ionization gap, 3 consequtive GEM foils separated by transfer gaps and a readout Printed Circuit Board (PCB), separated from the bottom GEM by an induction gap. The design and general properties of multi-GEM detectors were discussed in details earlier [3,4,5,8]. Here we will concentrate mainly on the design of readout PCB and its influence on operation of the detector. In LHCb each tracking plane of the Inner tracking system has to provide position in horizontal direction with a precision of better than $\sim 200\mu$ to keep momentum resolution below 0.5%. In the vertical direction, position accuracy can be 10 times worse as it is needed only for pattern recognition. Thus a stereo readout is foreseen with an angle of 0.1 rad.

The first measurements performed with large size prototype with small angle stereo readout [3] showed that the basic limitation on signal to noise ratio was high strip capacitance of the PCB. In the case of [3] it was about 100 pF for 30 cm long strips.

The PCB for such a detector is produced in two layers separated one from the other by a 50μ kapton foil. Between metal strips of the top layer the kapton layer is etched out and the metal of bottom layer is opened. We propose to make zero degree strips at the top layer and small angle stereo strips and the bottom layer. The bottom strips have to be made in short sections parallel to the top ones with narrow "bridges" connecting the sections belonging to one bottom strip. Schematic drawing of this layout is shown in fig.1.

In such a layout the area of overlapping regions between top and bottom metal layers is reduced, thus minimizing the interstrip capacitance. Moreover, as the bottom and top strips are parralel, the sharing of induced charge between will be constant, and will not depend on the position along the strip. This is not the case for the layout in [3] where top strips were not parallel to those at the bottom.

In order to reduce further the interstrip capacitance the strips have to be made as narrow as possible. A natural limitation for the width is the feature size of the technology, that is about 50μ. Thus the width of the top strip was chosen as 60μ. The ratio of the strip widths is determined by the requirement to have the same signal to be induced on top and bottom strips. As top and bottom strips are separated by 50μ and signal is induced by charge moving from the last GEM through the induction gap, bottom strips have to be wider than the top ones. We used MAXWELL package to calculate the necessary ratio of widths and strip capacitances. The thickness of copper layers was

4

4 mm

Top strip – 0.06 mm
Bottom strip – 0.15 mm
Bridge – 0.05 mm

0.4mm
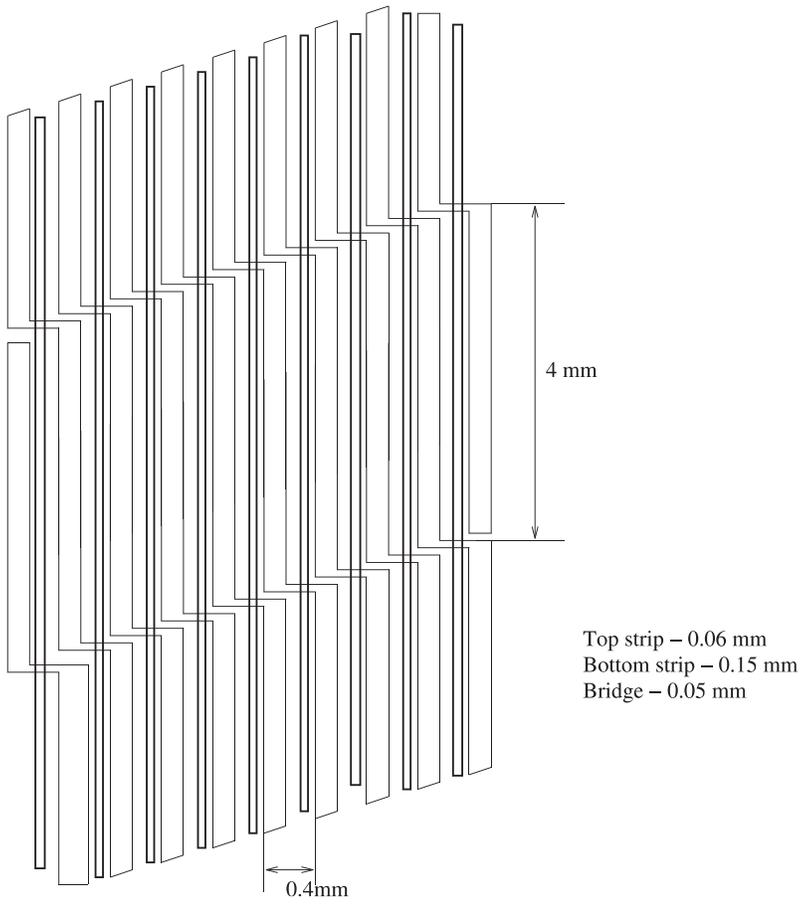
Figure 1: Schematic view of the PCB layout.

assumed to be 5μ. The kapton layer was 50μ thick and the width of kapton strip at the bottom was taken 10μ larger than at the top (at the contact with top strip). We also introduced in the model thick (1mm) epoxy substrate below the bottom strips. The calculations were made for a strip pitch of 400μ.

In the calculations we required that the ratio of the signals induced on the bottom strips with respect to the top ones is equal to 1.2, in order to compensate for the larger capacitance of the bottom strips. The results of the calculations are shown in table 1.

In order to achieve the sharing of induced signals as indicated above the width of the bottom strips has to be 150μ. The values of calculated strip capacitance per cm of length are shown in the first row of Table 1. The capacitance of the bottom strip is almost 2 times higher than that of top strip. However we can see that for 30cm long strip total capacitance will be below 20pF. In the second row of the table the results of measurements are shown. A $10 \times 19\,\text{cm}^2$ prototype PCB was used for the measurments with all strips grounded around the one which capacitance was measured. Experimental results are higher than calculated ones probably due to the differences in the particular shape of metal and kapton strip edges.

Table 1: Strip widths and capacitances for the optimized PCB.

layer	strip width	pF/cm (calculation)	pF/cm (measurement)
bottom	150μ	0.62	0.73
top	60μ	0.32	0.54

The prototype boards were produced with parameters shown in table 1 and size of sensitive area of $10 \times 10\,\text{cm}^2$. Top and bottom strips were extended from both sides forming very long bonding pads with a length of 4.5 cm and effective pitch of 200μ. Such long pads were made to have more freedom in connecting electronics, and simulate the case of a real strip length having smaller sensitive area.

The Triple-GEM detectors were assembled with prototype boards and GEM foils with $10 \times 10\,\text{cm}^2$ sensitive area. All transfer gaps were 1mm and induction gaps 2 mm. In the transfer and induction gaps we put bent strips of mylar 1mm and 2 mm wide respectively that were attached to the frame at both ends. These strips served as spacers keeping GEM foil at a precise distance from the PCB and from each other. The drift gap was kept as 3 mm.

Two detectors were equipped with PREMUX hybrid with 512 channels each. Detailed description of PREMUX can be found in [9]. Each channel

6

of PREMUX contains low-noise preamplifier, shaper and analogue buffer. Analog buffers can be readout sequentially through 1MHz multiplexer. Top and bottom strips were connected to the channels of PREMUX in series, i.e. each "stereo" channel was followed by a "straight" channel. The separation of signals from "stereo" and "straight" strips has been made off-line during data analysis.

In order to study the performance of the Triple-GEM detectors in high intensity hadron beams, assembled devices were exposed to the beam of 350 MeV pions at the proton cyclotron in Paul Scherrer Institute (PSI, Villigen, Switzerland). The beam was tuned to have maximum intensity of $\sim 10^4 \text{mm}^{-2}\text{s}^{-1}$. The width of the beam was ~ 9 cm (FWHM) and the height was ~ 5 cm. Total beam intensity within the area of the detectors $(10 \times 10 \, \text{cm}^2)$ was $6 \times 10^7 \text{s}^{-1}$. With this beam intensity we could measure discharge probablity below 10^{-11} with reasonable statistical significance in several hours.

A schematic layout of the set-up at the beam is shown in fig.2. The two detectors were attached to the bench as close as possible to each other between two scintillating counters. The counters were used for the measurements of gain and efficiency at low intensity. For these measurements the beam intensity was reduced down to $\sim 100 - 1000$ Hz. Coincidence of scintillating counters was used as a trigger that produced sample-and-hold signal for PREMUX. Analog signals from each strip of the detectors were stored in the buffers of PREMUX, readout and digitized by a sampling ADC and then stored in the computer. More detailed description of the Data Acquisition system (DAQ) for PREMUX can be found in [10].
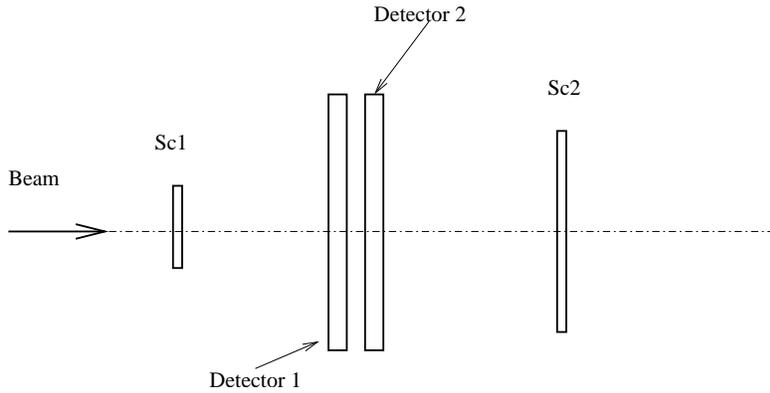
Figure 2: Schematic view of the set-up.

7

The correspondence between signal after the ADC and the input charge was found before the measurements using built-in calibration capacitances. With this electronic calibration we could determine input charge and gain of the detectors.

For counting of the discharges we measured the current of the drift cathode. In the presence of full beam intensity this current was higher than 1 nA when the gain was above 10^3. However when a discharge occured this current dropped to zero and then restored according to the recovery of GEM voltage. Using a current meter with analog output proportional to the input current, we assembled a simple set-up including an amplifier, discriminator and scaler. The threshold of this set-up was tuned in such a way that all the discharges were counted.
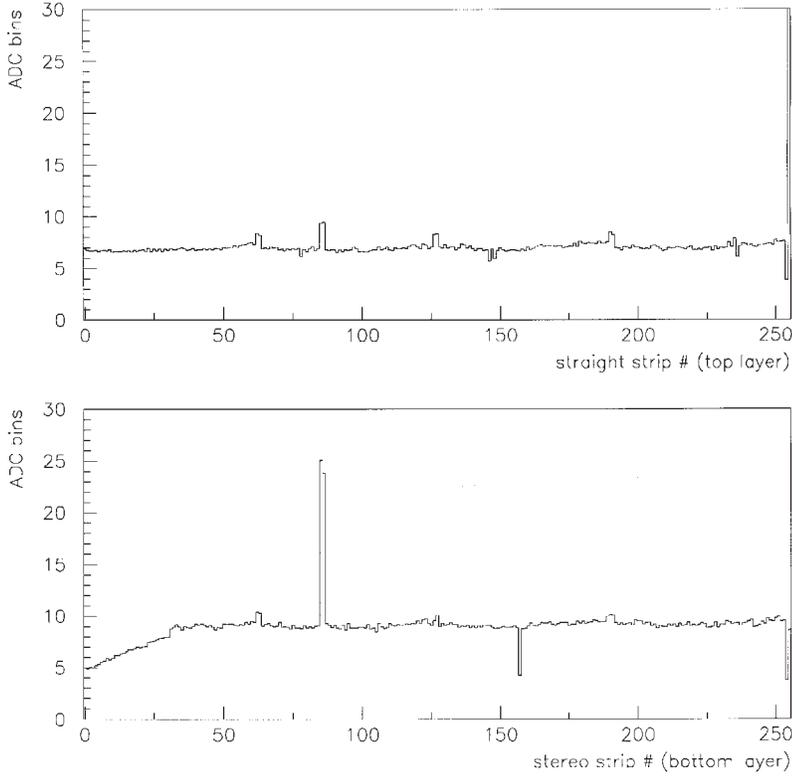
Figure 3: Noise values (sigma of gaussian fit) for all channels of the detector.
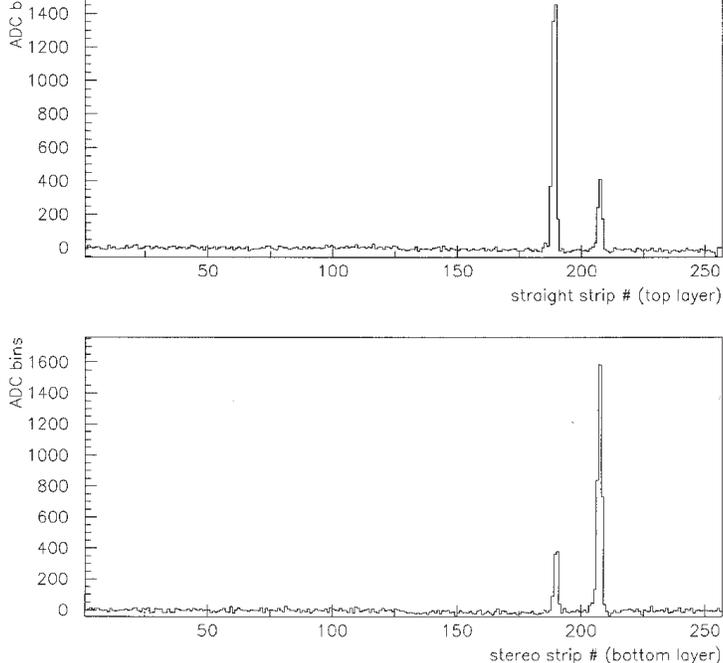
Figure 4: Typical signal from charged particle. Response of top and bottom layers is shown.

3 Results and discussion

The main goal of this work was to study the dependence of discharge probability on gas gain in the detector and compare it with the efficiency versus gain performance. The beginning of the efficiency plateau is determined by the primary ionisation deposited in the drift gap and noise of the electronics. In fig.3 noise values (sigma of the gaussian fit) are shown for all channels of one of the detectors, for straight strips (top figure) and stereo strips (bottom figure). We can see that the noise for stereo strips is higher (~ 9 ADC bins) than for straight strips (~ 6 ADC bins). From electronic calibration we knew that 1 ADC bin corresponded to 125 electrons. Thus the noise value for stereo channels was ~ 1200 e and for straight channels it was ~ 800 e. At the left side of the bottom figure we can see some reduction of the noise as stereo strips become shorter reaching the side edge of the structure rather than the opposite edge.

In fig.4 typical signals from charged particle are shown. Top and bottom

9

figures correspond to straight and stereo strips respectively. In both layers two groups of channels(clusters) have signals. Higher signal obviously corresponds to the main charge induced by the incident particle, while the smaller signal is a pick-up from the opposite layer. This conclusion is confirmed by coincidence of the smaller cluster position with the main one from the opposite layer. Such a strong pick-up is determined by very long extensions of the strips outside sensitive area where strips from both layers go parellel to each other. In the final detector such a design should be avoided and strips at the regions of fan-outs and bonding pads have to be as short as possible.

In order to find the cluster corresponding to an incident particle, first, all channels were sorted into straight and stereo ones. Then those channels that exceeded a certain threshold (usually 2-3 sigma noise) were found. Signals were summed up within continous groups of such channels (clusters). We took always only the cluster with the highest charge for further analysis. An example of cluster charge distribution is shown in fig.5. We can see clear separation of the main part of the signal from noise peak. Here the cluster signals from both layers were summed together.
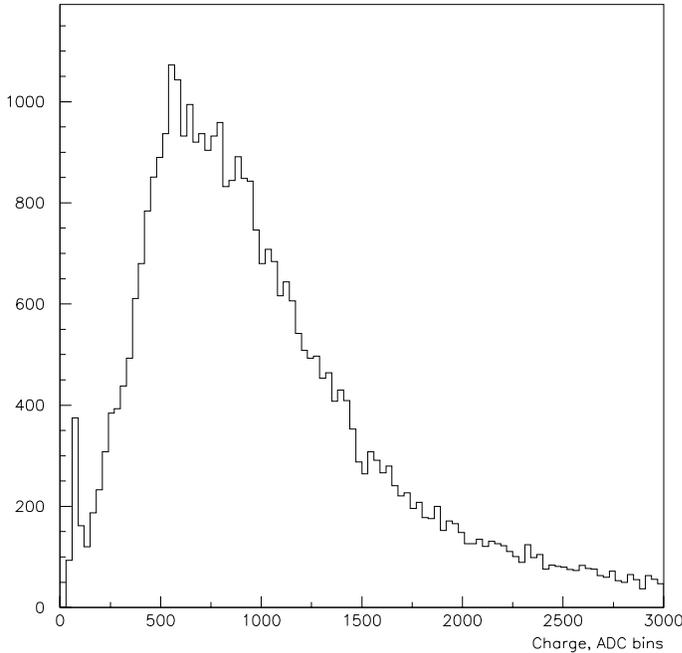
Figure 5: Typical cluster charge distribution.

10

The relationship between signals in top and bottom layers is shown in fig.6. Here the correlation between cluster charge in top and bottom layers is plotted. We see that these signals are almost equal to each other. Thus the result of this measurement is lower by 20% than the value expected from the calculations. Signals that are seen at the sides of the figure can appear when the main cluster is lost and the "pick-up" signal is taken instead. Losses of signal might happen due to two noisy and two broken channels in the bottom layer that were excluded from the analysis (see fig.3).
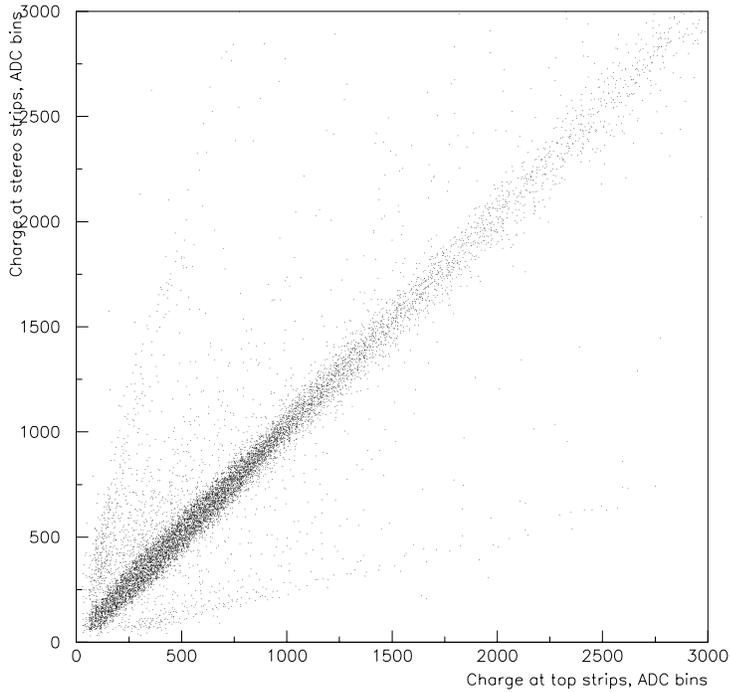
Figure 6: Correlation between cluster charge in top and in bottom layers.

The pion beam was tuned in such a way that most of the sensitive area of the detectors was irradiated. In fig.7 the distribution of reconstructed cluster positions in two dimensions is shown. This distribution demonstrates roughly the beam intensity within the area of the detector and scintillator counters. Binning in horizontal direction is determined by the spacing of straight strips (0.4 mm), while that in the vertical direction corresponds to the pitch of stereo structure (4 mm).

11
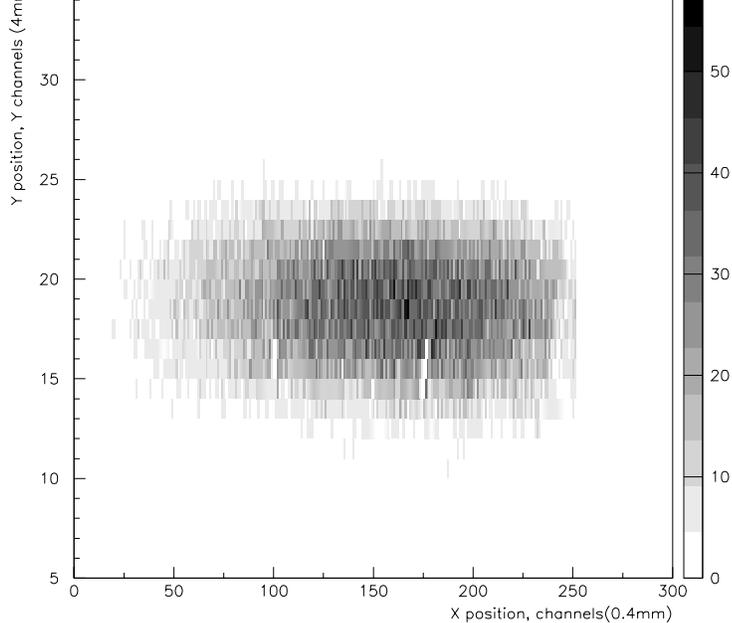
Figure 7: Beam profile measured at low intensity at detector 2.

Gas gain of the detectors was determined as the ratio of average cluster charge over the average number of primary electrons released by minimum ionising particle in the 3 mm gap. The latter is equal approximately to 30 electrons for the gas mixture used ($Ar-CO_2$, $70-30$). In fig.8 the dependence of gain on GEM voltage is shown for both detectors. Voltage differences from top to bottom electrodes in all GEMs were kept the same. The values of field in transfer, induction and drift gaps are indicated in the figure. The difference in gain at the same GEM voltage in two detectors can be explained by a limited precision of spacing of the GEM foils, accuracy of resistors in the resistive network and possible difference in hole diameter in different GEMs.

As we did not have any tracking devices apart from the detectors under study, we used one detector to determine the efficiency of the other. Efficiency of detector 2 was defined as the ratio of the number of cases when signals were found in both detectors to the total number of cases when detector 1 had a signal. With this definition of the efficiency we could not get values close to 100% because the detectors were not precisely aligned. Some tracks that were detected by detector 1 did not pass through detector 2. This problem

12
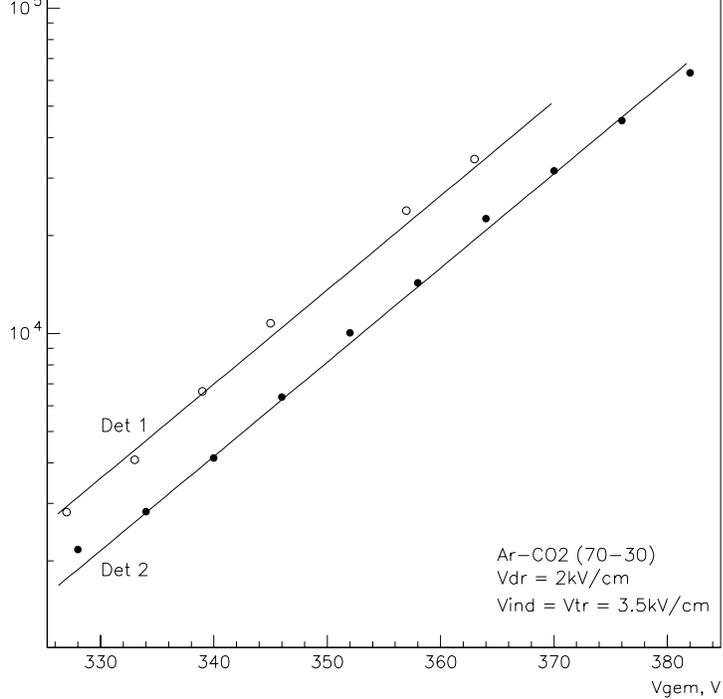
Figure 8: Dependence of gain on GEM voltage in two detectors.

however did not prevent to define the starting point of efficiency plateau. The dependence of efficiency on the gain together with the discharge probability is shown in fig.9. The values of efficiency are indicated at the left scale and the values of discharge probability at the right. The beginning of efficiency plateau is clearly determined at a gain of ~ 5000 while the value of probability equal to 10^{-11} is achieved at a gain of ~ 20000. There is a margin of a factor 4 between the beginning of efficiency plateau and discharge threshold where the detector can be operated safely.

13
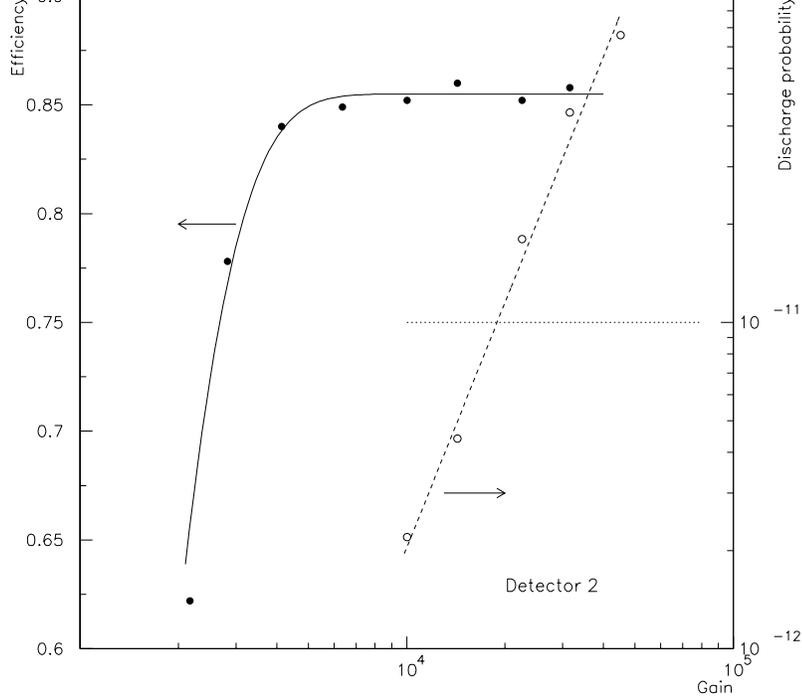
Figure 9: Dependence of efficiency (left scale) and discharge probability per incident particle(right scale) on gain. Dashed line is indicating the level of 10^{-11} considered as a safe limit.

4 Conclusions

Safe operation of the Triple-GEM detector was demostrated with a margin of a factor 4 between the beginning of efficiency plateau and gain where the discharge probability per incident particle exceeded 10^{-11}. The detector had a sensitive area of $10 \times 10 \, \text{cm}^2$ but the effective strip length was 19 cm. This result was possible due to an optimized design of the readout PCB that allowed significant reduction of the strip capacitance down to $0.5 - 0.7$ pF/cm. The detector still suffers from pick-up between the layers of PCB. In the final design the regions of fan-outs and bonding pads will be made as short as possible and this effect will be significantly suppressed.

14

References

[1] *A.Bressan et.al.* High rate behavior and discharge limits in micro-pattern gas detectors, NIM A, v.425 (1999), p.254-61.

[2] *F.Sauli* GEM: a new concept for electron amplification in gas detectors, NIM A, v.386 (1997), p.531-34.

[3] *M.Ziegler et.al..* A triple GEM detector with two dimensional readout, hep-ex/0007007, 4 Jul 2000.

[4] *S.Bachmann et.al.* Discharge study and prevention in the gas electron multiplier, CERN-EP-2000-151.

[5] *S.Bachmann et.al.* Performance of GEM detectors in high intensity particle beams, NIM A, v.470 (2001), p.548-61.

[6] *V.Talanov.* Radiation environment at the LHCb Inner Tracker area, LHCB-2000-013.

[7] *J.-P.Perroud.* Private communication, May 2000.

[8] *S.Bachmann et.al.* Charge amplification and transfer processes in the gas electron multiplier, NIM A, v.438 (1999), p.376-408.

[9] *L.Jones.* PreMUX specification V2.3, Rutherford Appleton Laboratory internal document, 1995.

[10] *A.Bondar et.al.* Tracking properties of the two-stage GEM/micro-groove detector, NIM A, v.454 (2000), p.315.